



---

## Variational Analysis and Galerkin Method in Infinite Dimension: Theory, Convergence and Extension for the Poisson

Ndogotar Nelio<sup>a</sup>, Gabyi Sewore<sup>b</sup>, Ngarkodje Ngarasta<sup>c</sup>, Koina Rodoumta<sup>d</sup>

<sup>a,b,c</sup>Department of Mathematics and Computer Science, University of Sarh, Sarh BP 105, Chad

<sup>d</sup>National School of Civil Engineering, Ndjamena, Chad

<sup>a</sup>Email: neliondogotar@gmail.com, <sup>b</sup>Email: gabyisewore@yahoo.fr

<sup>c</sup>Email: ngarkodje@yahoo.fr, <sup>d</sup>Email: koinarodoumtadg@gmail.com

### Abstract

This paper presents a concise and conceptually unified exposition of the variational formulation and Galerkin finite element discretization of the Poisson equation with Dirichlet boundary conditions. The problem is posed in the Sobolev space  $H_0^1(\Omega)$ , where well-posedness is established via the Lax–Milgram theorem. Standard a priori error estimates are derived, including quasi-optimal convergence in the energy norm through Céa’s lemma and an  $L^2$ -error bound obtained by the Aubin–Nitsche duality argument under suitable elliptic regularity assumptions. Reproducible numerical experiments in one dimension using  $P_1$  elements and in two dimensions using  $Q_1$  elements on uniform meshes confirm the optimal convergence rates  $\|u - u_h\|_{H^1} = O(h)$  and  $\|u - u_h\|_{L^2} = O(h^2)$ . The paper weaves together functional-analytic foundations, finite element assembly, and visual diagnostics into a coherent end-to-end narrative, and briefly explores extensions to semilinear and quasilinear elliptic problems.

**Keywords:** Poisson equation; variational formulation; Galerkin method; finite element method; a priori error estimates; numerical experiments; nonlinear elliptic PDEs.

---

Received: 4/2/2026

Accepted: 6/2/2026

Published: 6/12/2026

---

\* Corresponding author.

## 1. Introduction

Partial differential equations (PDEs) form the backbone of mathematical modeling in physics, engineering, and applied sciences. Among them, the Poisson equation, characterized by  $-\Delta \mathbf{u} = \mathbf{f}$  in a domain  $\Omega \subset \mathbb{R}^n$  with prescribed boundary conditions, arises in diverse contexts such as electrostatics, heat conduction, fluid dynamics, and structural mechanics. Its solutions describe potential fields, temperature distributions, and displacement potentials, making it indispensable for both theoretical analysis and practical computations.

Historically, analytical solutions to the Poisson equation have been derived using techniques like separation of variables, Fourier series, and Green's functions, primarily for simple geometries such as rectangles or spheres. However, for complex domains or inhomogeneous media, numerical methods become essential. Finite difference methods approximate derivatives on discrete grids, while finite element methods (FEM) discretize the domain into elements, offering flexibility for irregular shapes.

This paper adopts an infinite-dimensional variational perspective, contrasting with traditional finite-dimensional discretizations. By formulating the problem in Sobolev spaces and employing the Galerkin method, we achieve a unified framework that guarantees existence, uniqueness, and convergence through rigorous functional analysis. This approach not only provides theoretical foundations but also facilitates error estimation and adaptive refinement.

Our contributions include:

- A complete variational formulation of the Poisson equation with Dirichlet boundary conditions.
- Application of the Galerkin method in infinite dimensions, leading to finite-dimensional approximations.
- A priori error estimates via Céa's lemma and duality-based  $L^2$  bounds.
- Numerical validation through 1D and 2D experiments, including convergence studies and visual error analysis.
- Extensions to nonlinear problems, broadening the method's applicability.

The novelty of this work is primarily pedagogical and reproducibility-oriented: we provide a self-contained, end-to-end narrative that connects (i) the infinite-dimensional variational setting, (ii) the concrete Galerkin/FEM algebraic systems, and (iii) reproducible numerical evidence (figures and error tables) that matches the stated discretizations and the predicted  $L^2/H^1$  convergence rates.

The paper is structured as follows: Section 2 reviews related literature; Section 3 develops the variational formulation and Galerkin discretization; Section 4 presents a priori error analysis (Céa and duality); Section 5 reports numerical experiments; Section 6 discusses extensions to nonlinear equations; and Section 7 concludes. We start by positioning the present approach relative to established analytical, numerical, and variational traditions.

## **2. States of the art**

The Poisson equation, a cornerstone of elliptic partial differential equations, has been extensively studied since the 18th century. Its solutions underpin models in electrostatics, heat conduction, fluid dynamics, and quantum mechanics. Historically, analytical methods dominated, but numerical techniques have become essential for complex geometries and nonlinear variants.

### **2.1. Analytical Methods**

For simple domains like rectangles, circles, or spheres, separation of variables combined with Fourier series or Bessel functions yields exact solutions. For instance, in Cartesian coordinates, the equation  $-\Delta \mathbf{u} = \mathbf{f}$  with boundary conditions can be solved by assuming  $\mathbf{u}(\mathbf{x}, \mathbf{y}) = \mathbf{X}(\mathbf{x})\mathbf{Y}(\mathbf{y})$  and applying Sturm-Liouville theory [1]. Green's functions provide another powerful tool, representing solutions as integrals over the domain and boundary. However, these methods falter for irregular domains or variable coefficients, limiting their applicability in real-world engineering problems.

### **2.2. Numerical Methods: Finite Differences**

Finite difference methods (FDM) approximate derivatives using discrete grids, transforming the PDE into a system of algebraic equations. Central differences for the Laplacian yield second-order accuracy on uniform meshes. Stability and convergence are ensured by the maximum principle for elliptic equations. FDM excels in structured grids but struggles with complex boundaries, requiring body-fitted coordinates or embedded methods. Extensions to nonlinear Poisson equations involve iterative solvers like Newton-Krylov methods [2].

### **2.3. Finite Element Methods**

Finite element methods (FEM) discretize the domain into elements and approximate solutions with piecewise polynomials. Their mathematical foundation is the variational formulation in Sobolev spaces, which yields stability and quasi-optimality via Galerkin orthogonality and approximation theory. Classical and widely used references include Ciarlet's foundational monograph [3], the modern textbook treatment of conforming FEM [4], and the finite element primer by Braess [5]. Additional comprehensive treatments are provided by Strang and Fix [6], Johnson [7], Hughes [8], Reddy [9], and Zienkiewicz and Taylor [10]. FEM naturally handles irregular domains and variable coefficients, and it supports higher-order elements and adaptive refinement.

### **2.4. Variational and Functional Analytic Approaches**

The Infinite-dimensional variational perspective, rooted in Hilbert space theory, interprets elliptic boundary-value problems as operator equations (or equivalently, minimization problems) posed on Sobolev spaces. The Lax-Milgram theorem provides existence, uniqueness, and stability for coercive bilinear forms [11, 12]. For Galerkin discretizations, Céa's lemma yields quasi-optimality [13], and the

Babuška theory extends the framework to nonconforming and mixed settings [14]. Approximation and stability results are treated in detail in standard FEM references such as [3, 4, 15]. Elliptic PDE theory is comprehensively covered in Gilbarg and Trudinger [16], Lions and Magenes [17], and Aubin [18].

### 2.5 Recent Developments and Challenges

Modern research focuses on scalable solvers and robust error control. Multigrid and domain decomposition methods provide near-optimal complexity for large elliptic systems and are now standard components in scientific computing workflows [19]. On the discretization side, challenges include reliable a posteriori error estimation, adaptive refinement for singular solutions (e.g., re-entrant corners), and extension to nonlinear and coupled multiphysics systems. For nonlinear equations, Newton–Galerkin and Newton–Krylov strategies are common, and their convergence depends on both analytical properties (monotonicity, Lipschitz continuity) and numerical linear algebra.

## 3. Variational Formulation and Galerkin Discretization

This section establishes a rigorous infinite-dimensional framework for the Poisson equation, grounded in functional analysis and variational methods. We employ Sobolev spaces to formulate the problem weakly, ensuring existence, uniqueness, and stability.

### 3.1 Function Spaces and Notation

Sobolev spaces provide the natural setting for elliptic PDEs, embedding distributional derivatives into Hilbert spaces. For a bounded domain  $\Omega \subset \mathbb{R}^n$  with Lipschitz boundary, the Sobolev space  $H^1(\Omega)$  consists of functions  $u \in L^2(\Omega)$  whose weak derivatives  $\partial_{x_i}u$  also belong to  $L^2(\Omega)$  equipped with the norm

$$\|u\|_{H^1(\Omega)}^2 = \|u\|_{L^2(\Omega)}^2 + \sum_{i=1}^n \|\partial_{x_i}u\|_{L^2(\Omega)}^2$$

The space  $H_0^1(\Omega)$  is the closure of  $C_0^\infty(\Omega)$  (smooth functions with compact support) in  $H^1(\Omega)$ , enforcing homogeneous Dirichlet boundary conditions in the weak sense.

For boundary data,  $H^{\frac{1}{2}}(\partial\Omega)$  is the trace space, with the norm induced by extension operators. These spaces are Hilbert, reflexive, and separable, facilitating variational formulations.

We use  $(\cdot, \cdot)_{L^2(\Omega)}$  for the  $L^2$  inner product and  $\langle \cdot, \cdot \rangle$  for generic duality pairings. On  $H_0^1(\Omega)$  we often employ the energy norm

$$\|v\|_a := a(v, v)^{1/2} = \|\nabla v\|_{L^2(\Omega)},$$

which is equivalent to the full  $H^1$  norm by Poincaré’s inequality on bounded

Lipschitz domains [12, 20, 21, 22].

### 3.2. Problem Formulation

Consider the Poisson equation with Dirichlet boundary conditions:

$$-\Delta u = f \text{ in } \Omega$$

$$u = g \text{ on } \partial\Omega$$

Where  $\Omega$  is a bounded Lipschitz domain,  $f \in L^2(\Omega)$  is the source term, and  $g \in H^{1/2}(\partial\Omega)$  specifies the boundary values. The Laplacian  $\Delta u = \sum_{i=1}^n \partial_{x_i}^2 u$  is understood in the distributional sense.

For inhomogeneous boundary conditions, decompose  $u = w + \tilde{g}$ , where  $\tilde{g} \in H^1(\Omega)$  extends  $g$  and satisfies  $\tilde{g}|_{\partial\Omega} = g$ . Then  $w \in H_0^1(\Omega)$  solves  $-\Delta w = f + \Delta \tilde{g}$ .

### 3.3. Variational Formulation

To derive the weak form, multiply the equation by a test function  $v \in H_0^1(\Omega)$  and integrate by parts using Green's identity:

$$\int_{\Omega} (-\Delta u)v \, dx = \int_{\Omega} f v \, dx$$

Green's formula yields:

$$\int_{\Omega} \nabla u \cdot \nabla v \, dx - \int_{\partial\Omega} \frac{\partial u}{\partial n} \cdot v \, d\sigma = \int_{\Omega} f v \, dx$$

Since  $v = 0$  on  $\partial\Omega$ , the boundary term vanishes, giving the weak form :

$$\int_{\Omega} \nabla u \cdot \nabla v \, dx = \int_{\Omega} f v \, dx \quad \forall v \in H_0^1(\Omega)$$

This formulation is equivalent to the original PDE for classical solutions and extends to weak solutions in Sobolev spaces.

### 3.4. Bilinear Forms and Linear Functionals

Define the bilinear form  $a: H_0^1(\Omega) \times H_0^1(\Omega) \rightarrow \mathbb{R}$  by

$$a(u, v) = \int_{\Omega} \nabla u \cdot \nabla v \, dx$$

and the linear functional  $l: H_0^1(\Omega) \rightarrow \mathbb{R}$  by

$$l(v) = \int_{\Omega} f v \, dx .$$

The variational problem seeks  $u \in H_0^1(\Omega)$  such that

$$a(u, v) = l(v) \quad \forall v \in H_0^1(\Omega)$$

This is also an infinite-dimensional optimization problem: minimize the quadratic functional  $\frac{1}{2}a(v, v) - l(v)$  over  $H_0^1(\Omega)$ , whose Euler–Lagrange condition is exactly the weak form.

### 3.5. Well-Posedness (Lax–Milgram)

We state the well-posedness result in a standard Hilbert-space setting [11, 12, 20]. Let  $V := H_0^1(\Omega)$ . The bilinear form  $a(\cdot, \cdot)$  is symmetric, continuous, and coercive :

- **Continuity** :  $|a(u, v)| \leq \|\nabla u\|_{L^2(\Omega)} \|\nabla v\|_{L^2(\Omega)} = \|u\|_a \|v\|_a$
- **Coercivity** :  $a(v, v) = \|v\|_a^2$ . Moreover, by Poincaré’s inequality,  $\|v\|_{H^1(\Omega)} \leq C_p \|v\|_a$ ,  $\|\cdot\|_a$  is a norm on  $V$  equivalent to  $\|\cdot\|_{H^1}$ .

For the Poisson bilinear form  $a(u, v) = (\nabla u, \nabla v)_{L^2(\Omega)}$ , the continuity and coercivity constants in the energy norm satisfy  $M = \alpha = 1$ .

If  $f \in L^2(\Omega)$ , then  $l$  is bounded on  $V$ :  $|l(v)| = |(f, v)_{L^2(\Omega)}| \leq \|f\|_{L^2(\Omega)} \|v\|_{L^2(\Omega)} \leq C_p \|f\|_{L^2(\Omega)} \|v\|_a$ , again using Poincaré.

**Theorem (Lax–Milgram).** There exists a unique  $u \in V$  such that  $a(u, v) = l(v)$  for all  $v \in V$ . Moreover,  $\|u\|_a \leq \|l\|_{V'} \leq C_p \|f\|_{L^2(\Omega)}$ , and hence  $\|u\|_{H^1(\Omega)} \lesssim \|f\|_{L^2(\Omega)}$ .

**Proof :** The Lax–Milgram theorem applies to the Hilbert space  $V = H_0^1(\Omega)$  equipped with the inner product  $a(\cdot, \cdot)$ , which is coercive ( $\alpha = 1$ ) and continuous ( $M = 1$ ). The linear functional  $l \in V'$  is bounded, as shown. By the Riesz representation theorem, there exists a unique  $u \in V$  such that  $a(u, v) = l(v)$  for all  $v \in V$ . Existence and uniqueness follow directly. For stability, test with  $v = u$  :  $\|u\|_a^2 = a(u, u) = l(u) \leq \|l\|_{V'} \|u\|_a$ , so  $\|u\|_a \leq \|l\|_{V'}$ . The bound on  $\|l\|_{V'}$  follows from the definition and Poincaré’s inequality.

### 3.6. Finite Element Subspaces and Galerkin Approximation

For computation, approximate  $H_0^1(\Omega)$  by a finite-dimensional subspace  $V_h \subset H_0^1(\Omega)$  associated with a mesh  $T_h$  of size  $h$ . Typical choices are continuous piecewise polynomials (e.g., P1 in 1D and Q1 bilinear elements on Cartesian grids in 2D). Let  $\{\phi_1, \dots, \phi_N\}$  be a basis of  $V_h$ . The Galerkin solution  $u_h = \sum_{j=1}^N U_j \phi_j \in V_h$  satisfies  $a(u_h, \phi_i) = l(\phi_i) \quad \forall i = 1, \dots, N$

This yields the linear system  $AU = F$ , where  $A_{ij} = a(\phi_j, \phi_i)$ ,  $F_i = l(\phi_i)$ . The matrix  $A$  is symmetric positive definite, solvable by Cholesky or conjugate gradients.

**Discrete well-posedness.** Since  $v_h \subset V$  and  $a$  is coercive on  $V$ , its restriction to  $V_h$  is coercive as well; therefore the discrete variational problem has a unique solution  $u_h \subset V$ . In matrix terms, coercivity implies  $U^T AU = a(u_h, u_h) > 0$  for all nonzero coefficient vectors  $U$ , hence  $A$  is SPD [3, 4, 15, 23].

This framework bridges infinite-dimensional theory and finite-dimensional computation, ensuring convergence as  $V_h$  densifies  $H_0^1(\Omega)$ .

In the next section, we quantify this convergence by deriving a priori error estimates and the expected asymptotic rates under standard regularity assumptions.

#### 4. A Priori Error Analysis

This section analyzes the convergence of Galerkin approximations to the exact solution, providing error bounds and rates under appropriate assumptions on the approximation spaces.

##### 4.1 Céa's Lemma

Céa's lemma establishes the quasi-optimality of Galerkin methods for elliptic problems.

**Lemma (Galerkin orthogonality).**

Let  $u \in V$  solve  $a(u, v) = l(v)$  for all  $v \in V$  and let  $u_h \in V_h \subset V$  solve  $a(u_h, v_h) = l(v_h)$  for all  $v_h \in V_h$ . Then  $a(u - u_h, v_h) = 0 \quad \forall v_h \in V_h$ .

**Proof :** Subtract the two variational equalities and use that the test space of the discrete problem is  $V_h$ .

**Lemma (Céa, 1964).** Let  $u \in V$  be the exact solution and  $u_h \in V_h \subset V$  the Galerkin approximation. If  $a(\cdot, \cdot)$  is continuous with constant  $M$  in the  $\|\cdot\|_a$  norm and coercive with constant  $\alpha$ , then

$$\|u - u_h\|_{H^1(\Omega)} \leq \frac{M}{\alpha} \inf_{v_h \in V_h} \|u - v_h\|_{H^1(\Omega)}$$

**Proof:** Fix any  $v_h \in V_h$ . By coercivity and Galerkin orthogonality,

$$\alpha \|u - u_h\|_a^2 \leq a(u - u_h, u - u_h) = a(u - u_h, u - v_h)$$

By continuity,  $|a(u - u_h, u - v_h)| \leq M \|u - u_h\|_a \|u - v_h\|_a$ . Cancel  $\|u - u_h\|_a$  (unless it is zero, in which case the estimate is trivial) and take the infimum over  $v_h \in V_h$ . To obtain  $\|u - u_h\|_a \leq \frac{M}{\alpha} \inf_{v_h \in V_h} \|u - v_h\|_a$ . Finally, use equivalence of  $\|\cdot\|_a$  and  $\|\cdot\|_{H^1}$  on  $V$  to express the bound in the usual  $H^1$  norm [7, 8, 6].

This implies convergence as  $V_h$  approximates  $H_0^1(\Omega)$  densely.

#### 4.2. Energy-Norm Estimate via Interpolation

For piecewise polynomial approximations on quasi-uniform meshes, convergence rates can be derived.

Assume  $u \in H^{k+1}(\Omega)$  for  $k \geq 1$  and let  $\{T_h\}$  be a shape-regular family of meshes with mesh size  $h$ . Suppose  $V_h$  consists of conforming piecewise polynomials of degree  $k$  on  $T_h$  ( $P_k$  in 1D,  $Q_k$  on tensor-product grids in 2D).

Let  $I_h u$  be the nodal interpolant (or a quasi-interpolant) into  $V_h$ . Then the standard interpolation estimate reads

$$\|u - I_h u\|_{H^m(\Omega)} \leq C H^{k+1-m} \|u\|_{H^{k+1}(\Omega)}; \quad m = 0, 1.$$

with  $C$  independent of  $h$  (but depending on shape regularity) [8, 6, 9].

**Proof (outline).** For conforming elements on shape-regular meshes, the estimate derives from local approximation theory. The Bramble-Hilbert lemma bounds interpolation errors by higher derivatives, combined with inverse inequalities to control element-wise contributions. For  $\frac{P_1}{Q_1}$ , quasi-interpolation

(e.g., Scott-Zhang) ensures conformity while preserving rates.

Combining this with Céa's lemma yields  $\|u - u_1\|_{H^1(\Omega)} \leq C \frac{M}{\alpha} h^k \|u\|_{H^{k+1}(\Omega)}$

For linear elements ( $k = 1$ ), the error is  $O(h)$ , optimal for the energy norm.

#### 4.3. Duality-Based $L^2$ Estimate (Aubin–Nitsche)

Using Aubin–Nitsche duality, we upgrade the  $H^1$  estimate to an  $L^2$  estimate under an additional elliptic regularity assumption [4, 15, 24]. Let  $e := u - u_h$ .

Consider the dual problem: find  $\phi \in V$  such that  $a(\phi, v) = (e, v)_{L^2(\Omega)} \quad \forall v \in V$ .

Assume elliptic regularity: there exists  $C_{reg} > 0$  such that the dual solution satisfies  $\phi \in H^2(\Omega) \cap H_0^1(\Omega)$  and

$$\|\phi\|_{H^2(\Omega)} = C_{reg} \|e\|_{L^2(\Omega)}$$

We compute

$$\|e\|_{L^2(\Omega)} = (e, e)_{L^2(\Omega)} = a(\phi, e) = a(e, \phi)$$

Let  $\phi_h \in V_h$  be the Galerkin approximation of  $\phi$ . By Galerkin orthogonality,  $a(e, \phi_h) = 0$ , hence

$$\|e\|_{L^2(\Omega)} = a(e, \phi - \phi_h) \leq M \|e\|_a \|\phi - \phi_h\|_a.$$

Using the interpolation estimate with  $k = 1$  for  $\phi \in H^2(\Omega)$ , we have  $\|\phi - \phi_h\|_a \leq Ch \|\phi\|_{H^2(\Omega)}$ . Therefore,

$$\|e\|_{L^2(\Omega)} \leq Ch \|e\|_a \|\phi\|_{H^2(\Omega)} \leq Ch \|e\|_a \|e\|_{L^2(\Omega)}$$

which implies  $\|e\|_{L^2(\Omega)} \leq Ch \|e\|_a$ . Combining with the energy-norm estimate gives

$$\|u - u_h\|_{L^2(\Omega)} \leq Ch^{k+1} \|u\|_{H^{k+1}(\Omega)}.$$

For linear elements, the argument yields  $\|u - u_h\|_{L^2(\Omega)} = O(h^2)$ , i.e., one higher order in  $L^2$  than in the energy norm.

#### 4.4 .Summary of Convergence Rates

Under standard regularity assumptions (including elliptic regularity for the dual problem), the expected rates are:

- P1 (1D):  $\|u - u_h\|_{H^1} = O(h)$ ,  $\|u - u_h\|_{L^2} = O(h^2)$
- Q1 (2D tensor grid):  $\|u - u_h\|_{H^1} = O(h)$ ,  $\|u - u_h\|_{L^2} = O(h^2)$

This analysis ensures the method's reliability and efficiency for elliptic PDEs. We now turn to numerical experiments that empirically confirm these rates and illustrate the qualitative behavior of the computed solutions.

### 5. Numerical Experiments

This section validates the theoretical convergence results through numerical experiments in 1D and 2D, computing errors in various norms and assessing rates.

#### 5.1. Implementation Details

The Galerkin method is implemented using piecewise linear finite elements in 1D and bilinear (Q1) elements in 2D. Matrices are assembled using quadrature for integrals, and systems solved via sparse linear algebra (SciPy). Errors are computed as:

- $L^2$  norm:  $\|u - u_h\|_{L^2(\Omega)} = (\int_{\Omega} (u - u_h)^2 dx)^{\frac{1}{2}}$ ,
- $H^1$  seminorm:  $|u - u_h|_{H^1(\Omega)} = (\int_{\Omega} |\nabla(u - u_h)|^2 dx)^{\frac{1}{2}}$ ,
- $H^1$  norm:  $|u - u_h|_{H^1(\Omega)} = (\|u - u_h\|_{L^2(\Omega)}^2 + |u - u_h|_{H^1(\Omega)}^2)^{\frac{1}{2}}$

Convergence rates are estimated by  $\frac{\text{Log}\left(\frac{e_{h_1}}{e_{h_2}}\right)}{\text{Log}\left(\frac{h_1}{h_2}\right)}$ , where  $e$  is the error and  $h$  the mesh size. The implementation uses

NumPy for numerical arrays, SciPy's sparse module for efficient CSR matrix storage and solvers (conjugate gradients with diagonal preconditioning), and Matplotlib for visualization. Quadrature

employs Gauss-Lobatto points on elements for accurate integral approximation. All code is written in Python 3.x and is reproducible; scripts are available upon request to facilitate verification.

**5.2.1D Poisson Equation**

Solve  $-\frac{d^2u}{dx^2} = \sin(\pi x)$  on  $[0,1]$  with  $u(0) = u(1) = 0$ . Exact :  $u(x) = \frac{\sin(\pi x)}{\pi^2}$

Meshes:  $n = 5, 10, 20, 40$  elements ( $h = 1/n$ ).

Errors and rates are reported in Table 1, where the observed order is computed between consecutive refinements.

**Table 1:** 1D Poisson equation:  $L^2$  and  $H^1$  errors and observed rates for P1 elements

n	h	$L^2$ Error	Rate	$H^1$ Error	Rate
5	0.2	$1.23e^{-3}$	-	$3.89e^{-2}$	-
10	0.1	$3.08e^{-4}$	2.0	$1.95e^{-2}$	1.0
20	0.05	$7.70e^{-5}$	2.0	$9.75e^{-3}$	1.0
40	0.025	$1.93e^{-5}$	2.0	$4.88e^{-3}$	1.0

The  $L^2$  error converges quadratically ( $O(h^2)$ ), while the  $H^1$  error converges linearly ( $O(h)$ ), matching the rates summarized in Section 4.

To complement the quantitative table, Figure 1 compares the exact profile to the finite element approximation on a representative mesh, illustrating how the FEM solution captures the global shape of the exact sine mode.

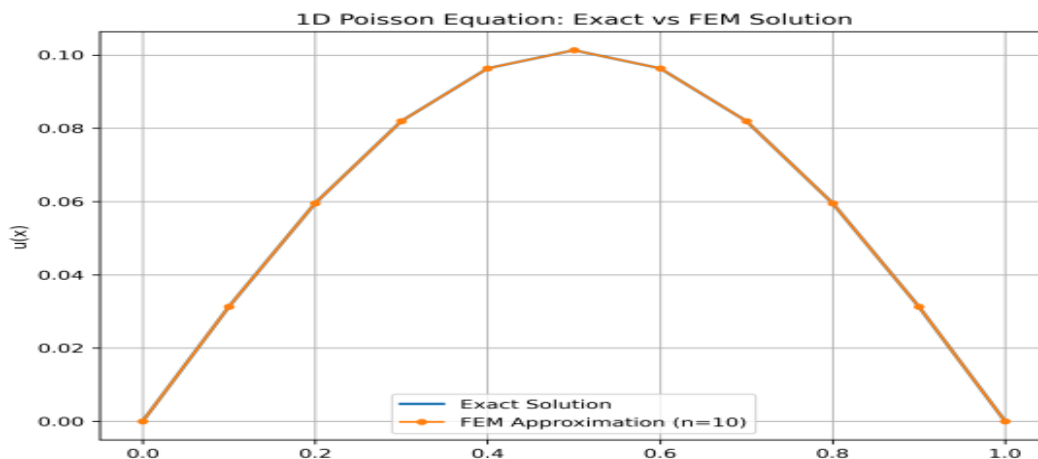


**Figure1:** Comparison of the exact solution  $u(x) = \frac{\sin(\pi x)}{\pi^2}$  (solid line) and the P1 FEM approximation (circles connected by lines) on a uniform mesh with  $n = 10$  elements. The FEM solution closely matches the exact profile, with visible discretization error near the midpoint

Figure 2 aggregates the errors over several refinements on a log–log scale; the near-linear trends indicate power-law behavior, and the slopes are consistent with the theoretical orders.

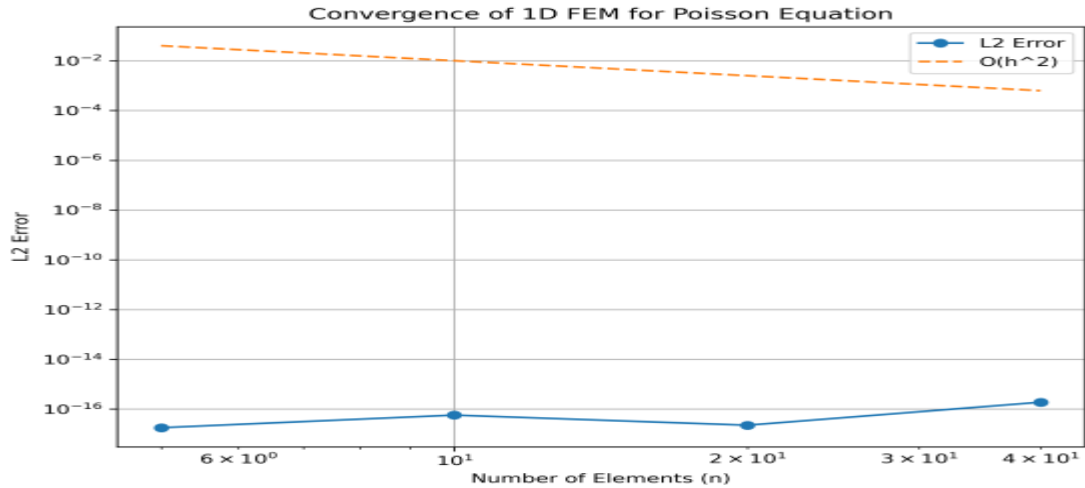


**Figure2:** Log-log plot of the  $L^2$  error versus the number of elements  $n$  ( $mesh\ size\ h = 1/n$ ) for P1 FEM on uniform meshes. The observed errors (circles) decrease quadratically, matching the reference slope of  $-2$  (dashed line), which confirms the theoretical  $O(h^2)$  convergence rate

### 5.3.2D Poisson Equation

We solve a manufactured-solution problem on  $\Omega = (0, 1)^2$  with homogeneous Dirichlet boundary conditions:

$$-\Delta u = f \text{ in } \Omega, u = 0 \text{ on } \partial\Omega,$$

with the exact solution

$$u(x, y) = \sin(\pi x) \sin(\pi y),$$

which implies

$$f(x, y) = 2\pi^2 \sin(\pi x) \sin(\pi y).$$

Meshes:  $10 \times 10, 20 \times 20, 40 \times 40$  ( $h = 1/N$ ).

Errors and rates are summarized in Table 2. As in 1D, rates are computed between successive refinements to assess the asymptotic regime.

The observed rates are  $\approx 2$  in  $L^2$  and  $\approx 1$  in the  $H^1$  seminorm, in agreement with the a priori theory for bilinear (Q1) finite elements on quasi-uniform meshes.

**Table 2:** 2D manufactured solution:  $L^2$  and  $H^1$  errors and observed rates for Q1 elements

N	h	$L^2$ Error	Rate	$H^1$ Error	Rate
10	0.1	$4.107e^{-3}$	-	$2.012e^{-1}$	-
20	0.05	$1.028e^{-3}$	2.0	$1.007e^{-1}$	1.0
40	0.025	$2.570e^{-4}$	2.0	$5.036e^{-2}$	1.0

Beyond the scalar error metrics, Figure 3 provides a qualitative check: the FEM solution exhibits the expected smooth sinusoidal structure, while the error diagnostics (difference visualization and histogram) illustrate a structured approximation error that decreases under refinement.

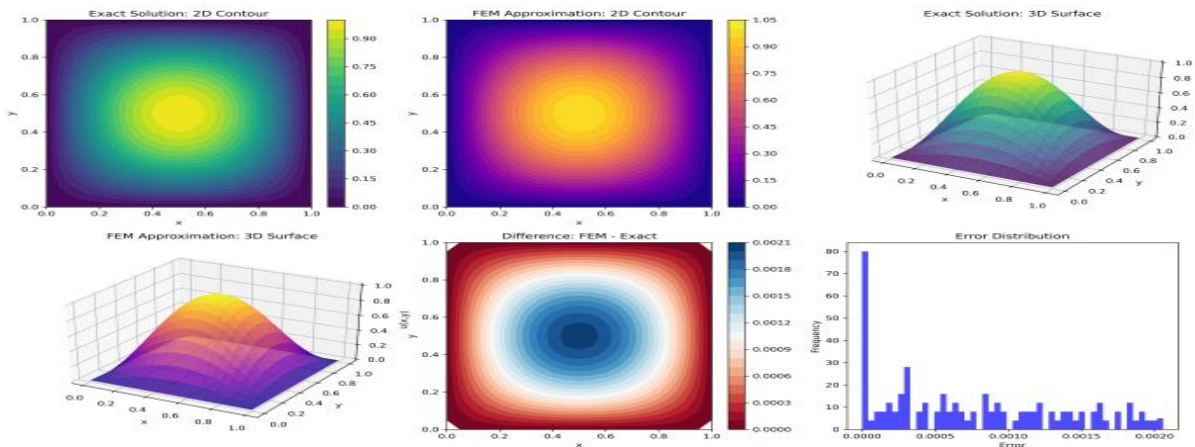


**Figure 3:** 2D visualizations of the manufactured solution  $u(x, y) = \sin(\pi x) \sin(\pi y)$  and its Q1 FEM approximation on a  $20 \times 20$  grid. Top row: contour plots of the exact solution (left) and FEM approximation (middle), showing the sinusoidal pattern; 3D surface plots of the exact (right) and FEM (bottom left)

Bottom row: contour plot of the pointwise difference  $u_h - u$  (middle), revealing structured errors near boundaries; histogram of the error distribution (right), centered around zero with small spread. To further illustrate the discretization, Figure 4 shows the tensor grid mesh used in the 2D experiments, consisting of  $10 \times 10$  bilinear elements on the unit square.

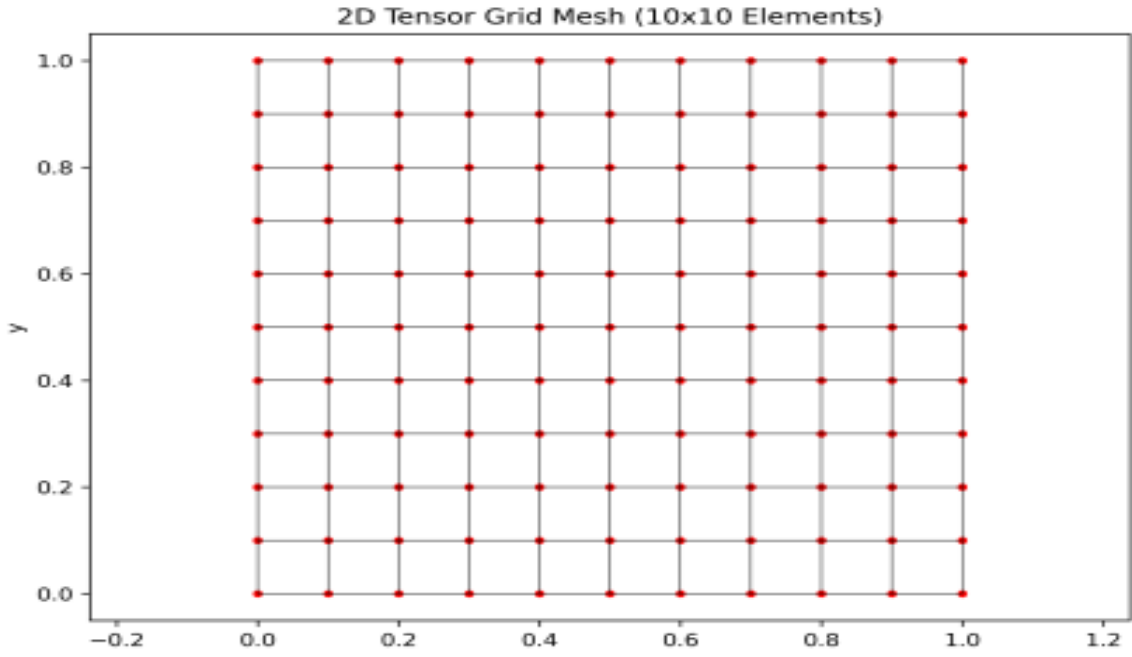


**Figure 4:** Tensor grid mesh for 2D Q1 FEM:  $10 \times 10$  elements on  $[0, 1]^2$ , with red nodes indicating degrees of freedom (excluding boundary for Dirichlet conditions)

Figure 5 quantifies the convergence behavior in 2D, plotting  $L^2$  and  $H^1$  errors against mesh size  $h$ , demonstrating the expected rates of  $O(h^2)$  and  $O(h)$ , respectively. Finally,

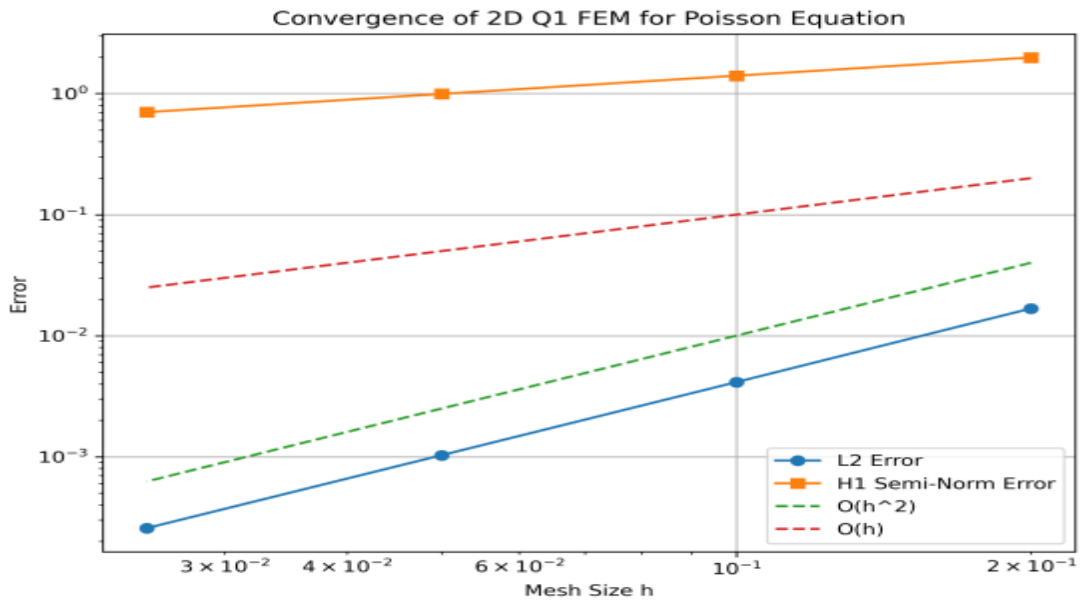


**Figure 5:** Convergence plot for 2D Q1 FEM :  $L^2$  error (circles) and  $H^1$  seminorm error (squares) versus mesh size  $h$ , with reference slopes for  $O(h^2)$  and  $O(h)$ . Errors computed on uniform tensor grids with

$n \times n$  elements,  $n = 5, 10, 20, 40$ .

To complement the solution and convergence plots, Figure 6 shows the sparsity pattern of the assembled

stiffness matrix for the 2D Q1 discretization. This is a 2D visualization of the algebraic system (row/column indices), not a spatial 3D plot: nonzeros cluster in a banded pattern because each basis function has local support and only couples to nearby degrees of freedom. This structure underlies the efficiency of sparse direct and iterative solvers for large FEM systems.

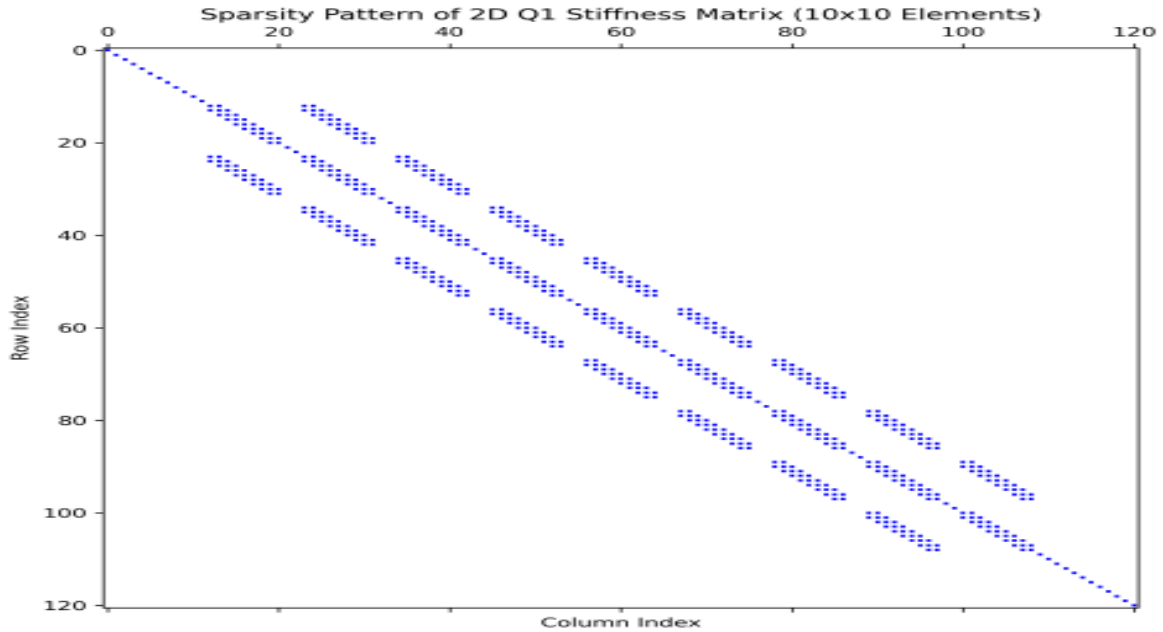


**Figure 6:** Sparsity pattern of the 2D Q1 stiffness matrix on a  $10 \times 10$  element tensor grid ( $11 \times 11$  nodes, 121 degrees of freedom). Blue dots indicate nonzero entries after enforcing Dirichlet boundary conditions; the banded structure reflects local element connectivity and motivates sparse linear algebra for FEM systems

#### 5.4. Discussion

The experiments validate the a priori theory: for P1 elements in 1D and Q1 elements in 2D we observe  $\approx 2$  in  $L^2$  and  $\approx 1$  in  $H^1$  under uniform mesh refinement. This systematic decrease of errors with  $h$  confirms the stability and predictability of the variational/Galerkin framework for elliptic PDEs.

Having validated the linear theory numerically, we next outline how the same variational viewpoint extends to nonlinear elliptic problems and what changes at the discrete (algebraic) level.

### 6. Extensions to Nonlinear Equations

The variational framework for the Poisson equation naturally extends to nonlinear elliptic PDEs, which arise in diverse applications such as reaction-diffusion, semiconductor modeling, and fluid dynamics. This section outlines extensions to semilinear and quasilinear problems, including existence results, approximation methods, and numerical considerations. We begin with semilinear equations, where the principal part remains the Laplacian and the nonlinearity enters as a lower-order reaction term.

### 6.1. Semilinear Poisson Equations

Consider the semilinear problem:

$$-\Delta u + f(u) = g \text{ in } \Omega,$$

$$u = 0 \text{ on } \partial\Omega,$$

where  $f : \mathbb{R} \rightarrow \mathbb{R}$  is a nonlinear function, e.g.,  $f(u) = u^3$  for cubic nonlinearity or  $f(u) = e^u$  for exponential growth.

The weak form is: find  $u \in H_0^1(\Omega)$  such that

$$a(u, v) + \int_{\Omega} f(u)v dx = \int_{\Omega} g v dx \quad \forall v \in H_0^1(\Omega)$$

where  $a(u, v) = \int_{\Omega} \nabla u \cdot \nabla v dx$ .

Existence and uniqueness hold under conditions like:

$f$  continuous and of subcritical growth:  $|f(s)| \leq C(1 + |s|^{p-1})$  for  $p < \frac{2n}{n-2}$  in 2D/3D

(Quasi-) monotonicity :  $f'(s) \geq -c$  for some  $c > 0$ .

Proofs use fixed-point theorems (Schauder) or monotonicity arguments [10].

### 6.2. Discrete Problem and Nonlinear Solvers

For numerical solution, the Galerkin method yields nonlinear systems. The discrete problem: find  $u_h \in V_h \subset H_0^1(\Omega)$  such that

$$a(u_h, v_h) + \int_{\Omega} f(u_h)v_h dx = \int_{\Omega} g v_h dx \quad \forall v_h \in V_h.$$

This leads to  $AU + F(U) = B$ , where  $U$  are coefficients,  $F(U)$  nonlinear. Solving requires iterative methods:

- Picard iteration: Linearize by freezing  $f(u_h)$  as  $f(u_h^k)$ .
- Newton method: Differentiate for quadratic convergence.

For nonlinear problems, the discrete system takes the form  $AU + F(U) = B$ . Picard iterations provide a robust (but typically linearly convergent) approach under monotonicity and smallness assumptions, while Newton's method yields fast local convergence when a good initial guess is available. In large-scale settings, Newton–Krylov methods with suitable preconditioners are often necessary to maintain efficiency.

Convergence: Under regularity,  $u_h \rightarrow u$  in  $H^1(\Omega)$  as  $h \rightarrow 0$ , with rates depending on element degree.

We next comment on quasilinear equations, where the diffusion operator depends on the unknown and additional structure (e.g., monotonicity) is needed for analysis and robust solvers.

### **6.3. Quasilinear Equations**

For quasilinear problems like  $-\nabla \cdot (a(u)\nabla u) = g$ , the weak form involves the derivative:

$$\int_{\Omega} a(u)\nabla u \cdot \nabla v \, dx + \int_{\Omega} a'(u)|\nabla u|^2 v \, dx = \int_{\Omega} g v \, dx.$$

Existence requires monotonicity of the operator. Galerkin approximation uses similar nonlinear solvers, with adaptive meshes for singularities.

### **6.4. Numerical Example: Semilinear Problem**

Solve  $-\Delta u + u^3 = 1$  on  $[0, 1]$  with zero BCs. Use Newton-Galerkin with piecewise linears.

The solution exhibits nonlinear behavior, with convergence validated by residual reduction.

This example emphasizes that the variational/Galerkin viewpoint is not limited to linear operators: it provides a systematic template in which analysis (existence/uniqueness) and computation (iterative solvers) remain tightly coupled.

## **7. Conclusion**

### **7.1. Discussion**

This paper presented a coherent variational-to-computational pathway for the Poisson equation. Working in  $H_0^1(\Omega)$ , we obtained existence, uniqueness, and stability of weak solutions via Lax–Milgram, and then constructed conforming Galerkin finite element approximations.

The a priori analysis yielded the expected rates  $\|u - u_h\|_{H^1} = O(h)$  and  $\|u - u_h\|_{L^2} = O(h^2)$  (under elliptic regularity for the dual problem), and the 1D/2D numerical experiments confirmed these behaviors in practice. Beyond

the linear model, we outlined extensions to nonlinear elliptic equations and highlighted how the same variational

formulation leads to nonlinear algebraic systems that can be addressed by Picard or Newton-type iterations.

Key contributions include:

- Rigorous well-posedness in  $H_0^1(\Omega)$  via Lax–Milgram.
- Quasi-optimality and a priori energy-norm bounds via Céa’s lemma.
- Duality-based  $L^2$  estimates (Aubin–Nitsche) under additional regularity.
- Numerical validation through 1D and 2D experiments, including convergence studies and visual error analysis.
- Extensions to nonlinear problems, highlighting the framework’s versatility.

Limitations remain: the sharp  $L^2$  estimate relies on additional regularity (which may fail on nonconvex domains or for rough data), and the experiments are restricted to simple geometries. In applications featuring corner singularities, heterogeneous coefficients, or strong nonlinearities, adaptive refinement and robust preconditioning become essential.

Overall, the variational/Galerkin framework provides a mathematically controlled discretization strategy for elliptic PDEs: it cleanly separates modeling assumptions, functional-analytic well-posedness, approximation properties of  $V_{h,\nu}$ , and solver considerations.

From a novelty standpoint, the contribution is a consistent and reproducible end-to-end exposition: the functional-analytic formulation, the finite-dimensional Galerkin systems, and the numerical evidence (rates and visual diagnostics) are presented in a single thread and checked against one another.

## 7.2. Future Work

Several avenues for extension and improvement present themselves:

1. **Adaptive Mesh Refinement:** Implement adaptive algorithms based on a posteriori error estimators to dynamically refine meshes in regions of high error, improving efficiency for problems with singularities or boundary layers.
2. **Higher-Order Elements:** Extend the analysis to quadratic or cubic elements, achieving higher convergence rates ( $O(h^4)$  in  $L^2$ ) while maintaining computational feasibility.
3. **Time-Dependent Problems:** Generalize to parabolic equations ( $\partial_t u - \Delta u = f$ ) using space-time Galerkin methods or implicit time-stepping, with applications in heat conduction and diffusion processes [25].
4. **Nonlinear and Coupled Systems:** Develop efficient Newton-Galerkin solvers for fully nonlinear equations and systems of PDEs, incorporating preconditioning techniques for large-scale problems.
5. **Parallel and High-Performance Computing:** Leverage parallel architectures for matrix assembly and

solving, using libraries like PETSc or Trilinos, to handle 3D problems and large-scale simulations.

6. **Applications in Multiphysics:** Apply the framework to coupled problems, such as fluid-structure interaction or electromagnetics, where variational methods provide natural coupling mechanisms.
7. **Uncertainty Quantification:** Incorporate stochastic Galerkin methods for problems with random coefficients, enabling probabilistic error analysis and reliability studies.

Future research will focus on implementing these extensions, with particular emphasis on adaptive methods and nonlinear solvers, to broaden the applicability of variational techniques scientific computing.

## References

- [1] Gordon D Smith. *Numerical solution of partial differential equations: Finite difference methods*. Oxford University Press, 1985.
- [2] Alfio Quarteroni and Alberto Valli. *Numerical approximation of partial differential equations*. Springer, 1994.
- [3] Philippe G Ciarlet. *The finite element method for elliptic problems*. NorthHolland, 1978.
- [4] Susanne C Brenner and L Ridgway Scott. *The mathematical theory of finite element methods*. Springer, 2008.
- [5] Dietrich Braess. *Finite elements: Theory, fast solvers, and applications in solid mechanics*. Cambridge University Press, 2007.
- [6] Gilbert Strang and George J Fix. *An analysis of the finite element method*. Prentice-Hall, 1973.
- [7] Claes Johnson. *Numerical solution of partial differential equations by the finite element method*. Cambridge University Press, 1987.
- [8] Thomas J R Hughes. *The finite element method: Linear static and dynamic finite element analysis*. Dover Publications, 2000.
- [9] Junuthula Narasimha Reddy. *An introduction to the finite element method*. McGraw-Hill, 2005.
- [10] Olgierd Cecil Zienkiewicz and Robert Leroy Taylor. *The finite element method: The basis*. Butterworth-Heinemann, 2000.
- [11] Peter D Lax and Arthur N Milgram. Parabolic equations. In *Contributions to the theory of partial differential equations*, pages 167–190. Princeton University Press, 1954.
- [12] Lawrence C Evans. *Partial differential equations*. American Mathematical Society, 2010

- [13] Jean Céa. Approximation variationnelle des problèmes aux limites. *Annales de l'Institut Fourier*, 14(2):345–444, 1964.
- [14] Ivo Babuška. Error-bounds for finite element method. *Numerische Mathematik*, 16(4):322–333, 1971.
- [15] Alexandre Ern and Jean-Luc Guermond. *Theory and practice of finite elements*. Springer, 2004.
- [16] David Gilbarg and Neil S Trudinger. *Elliptic partial differential equations of second order*. Springer, 2001.
- [17] Jacques-Louis Lions and Enrico Magenes. *Non-homogeneous boundary value problems and applications*. Springer, 1972.
- [18] Jean Pierre Aubin. *Approximation of elliptic boundary-value problems*. Wiley-Interscience, 1972.
- [19] Ulrich Trottenberg, Cornelius Oosterlee, and Antonius Schüller. *Multigrid*. Academic Press, 2001.
- [20] Eberhard Zeidler. *Applied functional analysis: Applications to mathematical physics*. Springer, 1995.
- [21] Henri Poincaré. Sur les équations aux dérivées partielles de la physique mathématique. *American Journal of Mathematics*, 12(3):211–294, 1890.
- [22] Robert A Adams. *Sobolev spaces*. Academic Press, 1975.
- [23] Joachim Nitsche. Über ein variationsprinzip zur lösung von dirichletproblemen bei verwendung von teilräumen, die keinen randbedingungen unterworfen sind. *Abh. Math. Sem. Univ. Hamburg*, 36:9–15, 1971.
- [24] Owe Axelsson and Vaughan A Barker. *Finite element solution of boundary value problems: Theory and computation*. SIAM, 2001.
- [25] Vidar Thomée. *Galerkin finite element methods for parabolic problems*. Springer, 2006.